CHALMERS

Hot Rolled Wire Descaling

Master's Thesis in Applied Physics

JON-HENRIK SVONNI

Department of Materials and Manufacturing Technology
CHALMERS UNIVERSITY OF TECHNOLOGY
Göteborg, Sweden 2012
Master's Thesis 2012:XX

MASTER'S THESIS

Hot Rolled Wire Descaling

Master's Thesis in Applied Physics
JON-HENRIK SVONNI

Department of Materials and Manufacturing Technology
CHALMERS UNIVERSITY OF TECHNOLOGY

Göteborg, Sweden 2012

Hot Rolled Wire Descaling
JON-HENRIK SVONNI

Master's Thesis
Department of Materials and Manufacturing Technology

Chalmers University of Technology
SE-412 96 Göteborg
Sweden
Telephone: + 46 (0)31-772 1000

Chalmers Reproservice
Göteborg, Sweden 2012

Hot Rolled Wire Descaling
Master's Thesis in Applied Physics
JON-HENRIK SVONNI
Department of Materials and Manufacturing Technology
Chalmers University of Technology

Abstract

In the process of making welding wire an important step is to descale an oxide layer from the surface of the wire. If the oxide layer is not entirely removed it will affect the quality of the finished product. A common way of descaling is to use acids which is not quite environmental friendly. It is possible to mechanically descale the wire but the method needs to be better since the current methods does not give consistent results.

In this work the possiblity to descale the wire using ultrasounds have been investigated. It has been theoretically analysed, modelled in MATLAB and compared with results from an existing mechanical wire descaler. The results have not been validated through experimental analysis.

The results show that ultrasound may be an interesting technique to investigate further, and guidelines and important variables for future experiments are given.

Contents

Abstract I

Contents III

Preface V

Notation VI

1 Introduction 1
- 1.1 Background . . . 1
- 1.2 Purpose . . . 1
- 1.3 Limitations . . . 1
- 1.4 Aim . . . 1
- 1.5 Layout . . . 1

2 Theory 2
- 2.1 Making Welding Wire . . . 2
  - 2.1.1 Stelmor cooling . . . 3
  - 2.1.2 Descaling . . . 3
  - 2.1.3 Coating and Drawing . . . 3
- 2.2 Ultrasonic Cleaning . . . 4
- 2.3 Vibrating String . . . 5
- 2.4 Discretizing the Wave Equation . . . 7
  - 2.4.1 Matrix Representation . . . 8
- 2.5 Acoustic Pressure . . . 8
- 2.6 The Wire Roll . . . 10
- 2.7 The Bending Moment . . . 10
- 2.8 Maximum Bending Momentum in the Elastic Region . . . 11

3 Method 13

4 Results 15
- 4.1 Length and Tension Dependencies . . . 15
- 4.2 Model Eigenfrequencies . . . 18
- 4.3 Maximum Bend for Elastic Region . . . 20
- 4.4 Wave Equation Simulations . . . 21
  - 4.4.1 The Frequency . . . 22
  - 4.4.2 Constant F . . . 23
  - 4.4.3 Constant p . . . 25
  - 4.4.4 Constant l . . . 27
  - 4.4.5 Matrix Size . . . 28

5 Discussion 29
- 5.1 Length and Tension Dependencies . . . 29
- 5.2 Model Eigenfrequencies . . . 29
- 5.3 Maximum Bend for Elastic Region . . . 29
- 5.4 Matrix Size . . . 29

5.5 The Results from Constant F, p and l 29
5.6 The Acoutic Pressure 30

6 Conclusion **31**
6.1 Future Work 31

Preface

This M.Sc. thesis has been conducted at ESAB Sweden and at Chalmers University of Technology at the department of Materials and Manufacturing Technology in the fall of 2011.

Acknowledgements

I would like to thank: Lars Nyborg at Chalmers University of Technology that has been the examiner of this master's thesis. Dean Ward and Jiri Hejcl at ESAB that have been my supervisors. I want to thank Peter Olsson, Lennart Josefsson and Håkan Wirdelius and the NDT group at Chalmers University of Technology for ideas and help during the project, and also Joel Kim at ESAB for support and feedback.

I also want to thank my family for all support throughout my time at Chalmers.

Göteborg March 2012
Jon-Henrik Svonni

Notations

M – Bending momentum [Nm]

T – Tension [N]

E – Young's modulus [N/m^2]

I – Second moment of area [m^4]

ρ – Density [kg/m^3]

A – Area [m^2]

L – Length [m]

ω – Angular frequency [rad/s]

P_{ac} – Acoustic power [W]

p – Sound pressure [Pa]

c – Sound velocity [m/s]

F – Force [N]

f – Frequency [Hz]

n – Eigenfrequency number

1 Introduction

1.1 Background

Removing an oxide layer from the surface of welding wires is necessary in MAG (Metal Active Gas) production before the wire drawing process. The present method is not quite environmental friendly because the usage of acids. When mechanically removing the scales some sticky remain. These can also be removed by mechanical descaling but the results are not consistent but depend on the operator.

There are several different mechanical descalers today. An example is wire rolls: The welding wires are drawn over the rolls and the bending momentum makes the oxide scales on the wire surface crack and fall off since they are less formable than the steel wire, but the method is however not perfect. A suggested technique is to use ultrasonic vibrations to achieve a similar bending momentums for better controllability and output.

1.2 Purpose

A need to investigate possible solutions for cleaner and quicker processes with better environmental control in the wire descaling process has been identified. The method needs to be efficient and consistent.

1.3 Limitations

The work is limited to an analytical and computational analysis and does not include experimental validations. In the simulations the wire is assumed to be elastic. Ultrasonics have been identified as a principle of interest and the work has been limited to only investigate this.

1.4 Aim

This project will start with an investigation of current options to define the direction of new technology and process in Hot rolled wire descaling. The process will be demonstrated with MATLAB analysis to evaluate the theory and practice. The object of the project is to obtain a process modification for a cleaner, quicker and better environmental control during the process.

It has been suggested that by vibrating the wire at eigenfrequency to make it resonate could produce large enough vibrations to produce a bending momentum that pops off the oxide scales. The eigenfrequencies of a wire that is held in both ends have been been calculated and the wire vibrations when subjected to a harmonic force at the eigenfrequency have been analysed through simulations.

1.5 Layout

The report is divided into six parts. After the introduction all theory needed for the understanding of the subsequent sections is given. In the others, the method is described, the results are presented, they are discussed and lastly conclusions from them are made.

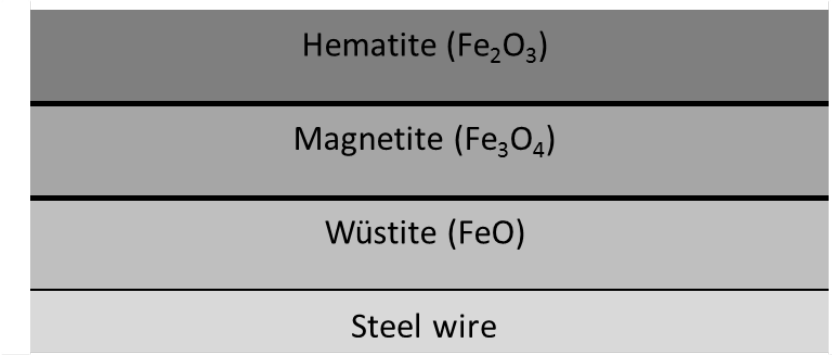

Figure 2.1: *Oxide layers formed on the wire.*

2 Theory

In this section the production of welding wire is described, then a subsection on ultrasonic cleaning follows, a technique mainly used for cleaning metal parts. It uses cavitational effects that comes from applying ultrasonics to a fluid-filled tank for cleaning.

The eigenfrequency calculations are shown in the subsection *Vibrating String*, then the discretization needed to simulate the displacements in MATLAB described. *Acoustic Pressure* connects the force in the calculations with actual force generated by pressure from ultrasound generators.

The Wire Roll section describes the mechanical descaling process that has been compared with the vibrating string. There are experimental data showing what diameter of the wire roll that is optimal for what wire diameter. This has been used in calculating what bending moment it produces. The bending moment on the wire, depending on the amplitude of vibrations and what eigenmode that is excited, is also calculated. Lastly the maximum allowed bending moment for the elastic region for the vibrating wire is also calculated.

2.1 Making Welding Wire

In the production of making wire the steel needs to be cooled, descaled, coated and produced for wet- or dry drawing.

The wire is made and coiled in a steel mill. This is done by processing the steel through several steps. An important step in the process is the coolng of the wire. When the wire is cooled, layers of iron oxide, forms on the surface, something that always will happen. The oxide consist of wüstite (FeO), magnetite (Fe_3O_4) and hematite (Fe_2O_3), see figure 2.1, and must be removed for the later wire drawing processes. This is commonly done using chemicals with the disadvantage of not being quite environmental friendly.

One way to cool the wire is *Stelmor cooling* which has been successful of making the surface of the wire more even and having the same properties over the whole length of the wire. This has made the wire drawing and also the chemical- and mechanical descaling of the wire easier.[1]

2.1.1 Stelmor cooling

In the Stelmor cooling process the wire initially gets cooled in water until the temperature of the wire drops from 950 C°, after this the wire is cooled in air to room temperature. The laying temperature i.e. the temperature in which the air cooling starts can be adjusted between about 875-750 C° and is very important for formation of different grain sizes and structure. The cooling can also be slow or delayed with different handling of the wire.[1]

A study to investigate the formation of oxide depending on the cooling conditions of high carbon wire rods have been conducted in laboratory simulations. During mechanical descaling the hematite layer is difficult to remove and tends to stick to the surface. This layer has been shown to be significantly thinner with higher laying head temperature and faster cooling. At high temperatures, only wüstit and magnetite are stable. Hematite forms as a decomposition of the high temperature oxides. If the cooling is fast less hematite is formed since there is less time for the oxides to decompose. Wüstit and magnetite are less adherent by nature and are therefore preferable. By keeping the laying head temperature close to 880 C° the hematite layer can be kept at a minimum. This was also reviewed and confirmed in a test plant.[2]

2.1.2 Descaling

The oxide scales that are formed on the wire during the cooling needs to be removed in order for the coating to stick in the next process step. This is usually done by acids or by mechanically removing them.

Chemical Descaling

When chemically removing the scales with sulfuric acid (H_2SO_4) or hydrochloric acid (HCl) the acid penetrates the scales in cracks and attacks the wüstite which is solvable in acids. The outer oxide layers are unaffected by the acid but gets undermined and therefore falls off. The environmental effects associated acids makes it interesting to evaluate mechanical descaling.[1]

Mechanical Descaling

There are several different ways of mechanically removing the scales. One method is called scale breaking. The wire is bent over rolls so that the outer fibers is stretched so much that the scales break and fall off while the more formable steel remains. Scale breaking always leaves some residues of the oxide and requires complementing methods to remove the rest. This can be done by brushing or by acids for instance. There are also several other techniques to remove the scales mechanically, like for instance by shot blasting, jet beam, shaving and with plasma.[1]

2.1.3 Coating and Drawing

After the descaling of the wire it gets coated and prepared for the drawing machine where the diameter of the wire is reduced to make welding wire.[1]

2.2 Ultrasonic Cleaning

Ultrasonic cleaning has existed for decades and is used in several different industries. It can for example remove oils, paints, dust and has also been successful of removing corrosion deposits from metals. The benefits from ultrasonic cleaning can be lowered labor costs, less time comsumption and more reliable cleaning.[3]

The set up consists of ultrasonic transducers connected to diaphragms, a generator and a tank filled with a cleaning liquid. The transducer is a piezo-ceramic material that changes its shape when it is excited by an electric signal. The piezo-electric transducer can be immersed into the tank. When it gets excited by an high frequency electric generator its vibrations get amplified by the diaphragm which causes compression and attenuation of the liquid in the tank. The liquid can be water or a cleaning chemical.[3]

The changes in density will start a cavitation process, bubbles will form and then implode. The frequency determines the magnitude of the bubbles. Low frequency produces larger bubbles than high frequency. The cavitation effect is more aggressive with increasing bubble size. The energy release from bubble implosions close to the surface destroys the contaminants, the implosion also creates a pressure wave and a high velocity jet and the cumulative effect of millions of implosions create the sufficient mechanical energy to break the contaminants bonds. The collapse of several cavities at the same time, clusters, may cause erosion of the sample.[3]

There are two mechanisms of ultrasonic cleaning, namely cavitation and acoustic streaming. When the cavitation bubbles implode they produce jets of liquid that can affect the surface to be cleaned. The cavitation takes place at discontinuities of the surface such as cracks and other features. The diameter of the bubbles are in the order of 100 μm at 25 kHz, and are generated on the order of microseconds with a estimated pressure of about 50 MPa. Instantaneous collapse pressures from clusters in the order of 1 GPa have been measured.[3]

In acoustic streaming the bulk liquid moves and the contaminants are carried away with it. Acoustic streaming is the dominating contribution of the cleaning at high frequencies, from about 170 kHz and even more over 1 MHz. At high frequencies the streaming velocities are greater and the cavitation bubbles are smaller. The shear stress from acoustic streaming is non-erosive and strongly adhered particles cannot be removed from surfaces, it does however help to flush away loosened particles from the surface.[3]

Two frequencies can be used simultaneously to clean a surface with improved effect. For example can a high and a low frequency combination make the surface cleaner than the sum of cleaning with both frequencies individually.[3]

2.3 Vibrating String

The mass of the wire is evenly distributed on the wire and the mass per unit length is ρ, the tension is T and when the wire is in rest it is on the x-axis. The wire is presumed to only move in the xu-plane.

For a string with the tension T applied in both ends the equation of motion of the string becomes 2.1.[4]

$$\frac{\partial^2 u}{dt^2} = c^2 \frac{\partial^2 u}{\partial x^2} - \beta^2 \frac{\partial^4 u}{\partial x^4} \tag{2.1}$$

$\beta = (\frac{EI}{\rho A})^{1/2}$, $c = (\frac{T}{\rho A})^{1/2}$, A is the cross-section area, ρ is the density, E is Young's modulus and I is the second moment of area about the x-axis.[4]

The moment of inertia about the length axis is calculated as 2.2, or in cylindrical coordinates 2.3. The second area of moment is through the center of a homogenous wire with radius a constant in the x-direction and is $I(x) = \frac{\pi a^4}{4}$.[5]

$$I_y(x) = \int_A z^2 \, \mathrm{d}A \tag{2.2}$$

$$I(x) = \int_0^a \int_0^{2\pi} r^2 sin^2(\phi) \, r \, \mathrm{d}r\mathrm{d}\phi \tag{2.3}$$

The equation of motion is solved with the separtion method to determine the eigenfrequencies of the wire, 2.4.

$$u(x,t) = X(x)T(t) \tag{2.4}$$

The separated equation of motion can now be solved. Since the X-equation and T-equation are independent of each other they must be equal to some constant λ, 2.5.

$$\beta^2 \frac{X^{(4)}(x)}{X(x)} - c^2 \frac{X''(x)}{X(x)} = -\frac{T''(t)}{T(t)} = \lambda \tag{2.5}$$

Because the solutions should be periodic λ must be positive. With $\lambda = \omega^2$ the solution of the T-equation 2.6, is 2.7.

$$T''(t) = -\omega^2 \, T(t) \tag{2.6}$$

$$T(t) = A_1 \sin \omega t + A_2 \cos \omega t \tag{2.7}$$

The X-equation 2.8 is solved by the ansatz $X(x) = B \, e^{s \, x}$ and solving the characteristic equation 2.9. This gives the solutions s_1 - s_4, 2.10.

$$X^{(4)}(x) - \frac{c^2}{\beta^2} X''(x) - \frac{\omega^2}{\beta^2} X(x) = 0 \tag{2.8}$$

$$s^4 - \frac{c^2}{\beta^2} s^2 - \frac{\omega^2}{\beta^2} = 0 \tag{2.9}$$

$$s^2 = \frac{c^2}{2\beta^2} \pm \sqrt{\frac{\omega^2}{\beta^2} + \frac{c^4}{4\beta^4}}$$

$$\Rightarrow \begin{cases} s_1 = \sqrt{\frac{c^2}{2\beta^2} + \sqrt{\frac{\omega^2}{\beta^2} + \frac{c^4}{4\beta^4}}} \\ s_2 = -\sqrt{\frac{c^2}{2\beta^2} + \sqrt{\frac{\omega^2}{\beta^2} + \frac{c^4}{4\beta^4}}} \\ s_3 = i\sqrt{\sqrt{\frac{\omega^2}{\beta^2} + \frac{c^4}{4\beta^4}} - \frac{c^2}{2\beta^2}} \\ s_4 = -i\sqrt{\sqrt{\frac{\omega^2}{\beta^2} + \frac{c^4}{4\beta^4}} - \frac{c^2}{2\beta^2}} \end{cases} \tag{2.10}$$

$s_1 = -s_2$ and $s_3 = -s_4$. Since s_3 is imaginary, s_3 will be the imaginary part from here on i.e. the root is is_3. The solution can be written as 2.11, this is modified to 2.13 through the relations 2.12.

$$X(x) = B_1\, e^{s_1\, x} + B_2\, e^{-s_1\, x} + B_3\, e^{is_3\, x} + B_4\, e^{-is_3\, x} \tag{2.11}$$

$$\begin{aligned} \sinh s_1\, x &= \frac{e^{s_1\, x} - e^{-s_1\, x}}{2} \\ \cosh s_1\, x &= \frac{e^{s_1\, x} + e^{-s_1\, x}}{2} \\ \sin s_3\, x &= \frac{e^{is_3\, x} - e^{-is_3\, x}}{2i} \\ \cos s_3\, x &= \frac{e^{is_3\, x} + e^{-is_3\, x}}{2} \end{aligned} \tag{2.12}$$

$$X(x) = B_1'\, \sinh s_1\, x + B_2'\, \cosh s_1\, x + B_3'\, \sin s_3\, x + B_4'\, \cos s_3\, x \tag{2.13}$$

The boundary conditions that the lateral movement and the moment in the ends are zero ($X(0) = 0$ and $X''(0) = 0$) gives that B_2' and B_4' has to be zero, 2.14.

$$\begin{cases} X(0) = B_2' + B_4' = 0 \\ X''(0) = s_2^2\, B_2' - s_4^2\, B_4' = 0 \end{cases} \tag{2.14}$$

The equation is now simplified to 2.15.

$$X(x) = B_1' \sinh s_1\, x + B_3' \sin s_3\, x \tag{2.15}$$

The conditions $X(L) = 0$ and $X''(L) = 0$ gives the equation system 2.16. Combing these gives 2.17. Multiplying the equations in 2.16 gives 2.18 and inserting 2.17 gives the relation needed for finding the eigenfrequencies.

$$\begin{cases} B_1'\, \sinh s_1\, L + B_3'\, \sin s_3\, L = 0 \\ s_1^2 B_1'\, \sinh s_1\, L - s_3^2 B_3'\, \sin s_3\, L = 0 \end{cases} \tag{2.16}$$

$$B_1' = -B_3' \frac{\sin s_3\, L}{\sinh s_1\, L} \tag{2.17}$$

$$\underbrace{s_1^2 B_1'^2 \sinh^2 s_1 L - s_3^2 B_3'^2 \sin^2 s_3 L}_{=(s_1^2+s_3^2)B_3'^2 \sin^2 s_3 L} + \underbrace{(s_1^2 - s_3^2)}_{=(\frac{c}{\beta})^2} B_1' B_3' \sinh s_1 L \sin s_3 L = 0 \tag{2.18}$$

The equation is satisfied for the relation 2.19.

$$s_3 L = n\pi, \quad n = ..., -2, -1, 0, 1, 2, ... \tag{2.19}$$

Inserting s_3 into 2.19 and simplifying gives the eigenfrequencies ω_n, 2.20.

$$\omega_n = \frac{n\pi\beta}{L}\sqrt{(\frac{n\pi}{L})^2 + (\frac{c}{\beta})^2}, \quad n = ..., -2, -1, 0, 1, 2, ... \tag{2.20}$$

The solution of the X-equation is the superposition for all values of n, 2.21. B' also depends on n.

$$X(x) = \sum_{n=-\infty}^{\infty} B_{1,n}' \sinh s_1 x + B_{3,n}' \sin s_3 x \tag{2.21}$$

Because of the relations 2.17 and 2.19, $B_{1,n}'$ becomes zero for all values of n. The total solution to the wave equation can now be written as, 2.22.[6;7]

$$u(x,t) = \sum_{n=-\infty}^{\infty} (\sin \frac{n\pi x}{L})(A_n \sin \omega_n t + B_n \cos \omega_n t) \tag{2.22}$$

2.4 Discretizing the Wave Equation

To simulate the vibrations to the wire when subjected to a harmonic force, the wave equation was discretized. The positions on the wire and the time is discretized with equation 2.23, 2.24 and 2.25.

$$x_j = j\Delta x; \quad j = 0, 1, 2, ..., J; \quad J\Delta x = L \tag{2.23}$$

$$t_n = n\Delta t; \quad n = 0, 1, 2, ..., N \tag{2.24}$$

$$u_j^n = u(x_j, t_n) \tag{2.25}$$

The wave equation can be written as 2.26 with F as 2.27.

$$\begin{aligned} \frac{u_j^{n+1} - 2u_j^n + u_j^{n-1}}{(\Delta t)^2} &= c^2 \frac{(u_{j+1}^n - 2u_j^n + u_{j-1}^n)}{(\Delta x)^2} \\ &\quad - \beta^2 \frac{(u_{j+2}^n - 4u_{j+1}^n + 6u_j^n - 4u_{j-1}^n + u_{j-2}^n)}{(\Delta x)^4} \\ &\quad + \frac{F(x,t)}{\rho A} \end{aligned} \tag{2.26}$$

$$F(x,t) = F_0(x) \cos \omega t \tag{2.27}$$

This gives the relation for the next time-step, 2.28.

$$\begin{aligned} u_j^{n+1} &= (2-2r^2-6r^2s^2)u_j^n - u_j^{n-1} \\ &\quad + (r^2+4r^2s^2)[u_{j+1}^n + u_{j-1}^n] \\ &\quad - r^2s^2[u_{j+2}^n + u_{j-2}^n] \\ &\quad + \frac{F(x,t)(\Delta t)^2}{\rho A} \end{aligned} \tag{2.28}$$

$r = \frac{c\,\Delta t}{\Delta x}$ and $s = \frac{\beta}{\Delta x}$.

2.4.1 Matrix Representation

The discretization was represented in a $J \times J$ matrix, 2.29. With the next time step as 2.30. The values of $\alpha - \epsilon$ are correspondin to equation 2.28 with $\alpha = \epsilon$, $\beta = \delta$. $\alpha = -r^2s^2$, $\beta = (r^2 + 4r^2s^2)$, $\gamma = (2 - 2r^2 - 6r^2s^2)$ and $\mathbf{B}$ is a diagonal matrix with the value -1 on all non-zero elements.

$$\mathbf{A} = \begin{pmatrix} \gamma & \delta & \epsilon & 0 & 0 & 0 & \dots \\ \beta & \gamma & \delta & \epsilon & 0 & 0 & \dots \\ \alpha & \beta & \gamma & \delta & \epsilon & 0 & \dots \\ 0 & \alpha & \beta & \gamma & \delta & \epsilon & \dots \\ \ddots & \ddots & \ddots & \ddots & \ddots & \ddots & \ddots \\ \dots & 0 & 0 & \alpha & \beta & \gamma & \delta \\ \dots & 0 & 0 & 0 & \alpha & \beta & \gamma \end{pmatrix} \tag{2.29}$$

$$u_j^{n+1} = \mathbf{A}u_j^n + \mathbf{B}u_j^{n-1} + \frac{F_0(x)(\Delta t)^2\,\cos\omega t}{\rho A} \tag{2.30}$$

The eigenfrequencies of the model with the matrix size $J \times J$ is determined by taking the square root of the eigenvalues calculated by using the MATLAB command `eig` on $\mathbf{A}$, and then plotted for increasing n to compare with the analytical eigenfrequencies.

2.5 Acoustic Pressure

A point source for acoustic pressure is used to determine what power the generator needs to have to achieve the needed force on the wire.

The sound power P_{ac}, for plane sound waves are given by equation 2.31. p is the sound pressure, A_s is the area of a sphere with the radius r from the point source, c_f is the velocity of sound in the medium and ρ_f is the density of given medium.

$$P_{ac} = \frac{p^2 A_s}{c_f \rho_f} \tag{2.31}$$

$A_s = 4\pi r^2$, this gives the equation for the sound pressure as 2.32. The sound pressure decreases with the distance with $1/r$.

$$p = \frac{1}{r}\sqrt{\frac{P_{ac}\,c_f\,\rho_f}{4\pi}} \tag{2.32}$$

The total force F added to the right hand side of the discretized wave equation 2.26 is the sum of the F_0 elements, 2.33. m is the number of elements that F is applied to.

$$F_{tot} = m\,F_0 \tag{2.33}$$

The total force is also the acoustic pressure times the area which is the length x multiplied by the diameter of the wire that the pressure is applied to, 2.34.

$$F_{tot} = pxd \tag{2.34}$$

Equation 2.33 and 2.34 gives the relation between the force used in the discretized wave equation and the pressure, see equation 2.35.

$$p = \frac{m\,F_0}{xd} \tag{2.35}$$

With the relations 2.35 and 2.32 it is possible to determine what power the generator needs to have and what distance it needs to have to the wire for a specified medium.

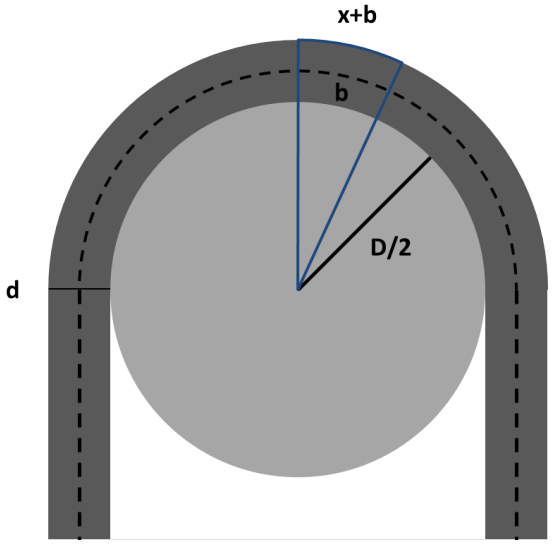

Figure 2.2: *The wire bent over a wire roll.*

2.6 The Wire Roll

When a wire is drawn over a roll the outer fibre is stretched and since the scales are less formeable than the wire, they will crack and fall off. Generally a fraction of the scales are more difficult to remove and must be removed afterwards. To evaluate the stretching required to remove the oxide wire drawing tests have been performed previously in a wire drawing machine. In tests a strain of about six percent is the goal for effective descaling.[1]

The strain of the wire over a roll is determined by the diameter of the wire and the roll. One can assume that the central line of the wire is unchanged over a distance b, then the outer fibre is enlongated with the distance x, as in figure 2.2. The elongation ϵ, in percent is given by the relation 2.36, with the diameter D for the roll and d for the wire.[1]

$$\frac{x+b}{b} = \frac{D/2+d}{D/2+d/2} \Rightarrow \frac{x}{b} = \epsilon = \frac{d}{D+d} \tag{2.36}$$

For a wire with the diameter of 5.5 mm and a roll with the diamter of 85 mm this becomes 6.08 %.

2.7 The Bending Moment

The relation between the bending moment and the radius of the bend is given by the relation 2.37.[5]

$$M = \frac{EI}{R} \tag{2.37}$$

For a wire of 5.5 mm on a wire roll of 85 mm the bending moment on the wire is 215 Nm.

The relation between the bending moment and the bend is given by the Euler-Bernoulli equation 2.38, also called the elastic line equation and the presumption is that the deformations in the wire are small, $\frac{du}{dx} \ll 1$ which is the case most times.[5]

$$M = -EI\frac{\mathrm{d}^2 u}{\mathrm{d}x^2} \tag{2.38}$$

The displacement of the wire is calculated before, in equation 2.22. It is therefore possible to derive it twice and calculate the bending moment at the point where the displacement is the largest, at C_{max}, 2.39.

$$M_{max} = EI\,(\frac{n\pi}{L})^2\,C_{max} \tag{2.39}$$

2.8 Maximum Bending Momentum in the Elastic Region

To determine how much the wire may be displaced and still be in the elastic region can be done by integrating the curve and plotting the result in MATLAB. The possible displacement is dependent on what wave mode is excited i.e. what n is used.

To do this the length of the wire in rest is compared with the wire when it has the amplitude C. Then it can be calculated for different frequencies. The wire has a sinusoidal curvature, 2.40. To evaluate it, x and y has to be expressed in the same variable, 2.41.

$$y(x) = C\sin\frac{n\pi x}{L} \tag{2.40}$$

$$\mathbf{r}(\theta) = (x(\theta), y(\theta)) \tag{2.41}$$

This is done with elliptical coordinates as in equation 2.42.

$$\begin{cases} y(\theta) = \frac{L}{2n}\sin\theta \\ x(\theta) = C\cos\theta \end{cases} \tag{2.42}$$

The length of a curve s is calculated with equation 2.43.[8]

$$s = \int_\Gamma \mathrm{d}s = \int_a^b |\dot{\mathbf{r}}(\theta)|\,\mathrm{d}\theta \tag{2.43}$$

Inserting 2.42 gives equation 2.44.

$$s = \int_0^{\pi/2} \sqrt{\dot{x}(\theta)^2 + \dot{y}(\theta)^2}\,\mathrm{d}\theta \tag{2.44}$$

After some simplifications this results in an elliptical integral 2.45, that needs to be solved with tabular values.[8]

$$s = \tfrac{L}{2n}\int_0^{\pi/2} \sqrt{1 - \underbrace{(1 - (\frac{C}{L/2n}))^2}_{k^2}\sin^2\theta}\,\mathrm{d}\theta \quad , (k^2 < 1) \tag{2.45}$$

The value $\frac{L}{2n}$ in front of the integral is the length of the wire in rest. So the value of the integral is therefore the elongation factor ϵ. The tabular values for different values of ϵ is listed with correspoding values for k is listed in 2.47. The k value for the different elongations is given by 2.46.

$$k = \sin\alpha \tag{2.46}$$

$$\begin{aligned} \epsilon = 1.01 \quad &\Rightarrow \quad \alpha = 85.6^\circ \\ \epsilon = 1.02 \quad &\Rightarrow \quad \alpha = 83.6^\circ \\ \epsilon = 1.03 \quad &\Rightarrow \quad \alpha = 81.6^\circ \end{aligned} \tag{2.47}$$

The amplitude C is used when calculating the bending moment. By combining k from equation 2.45 and 2.46 an equation for the maximum displacement for different elongations can be calculated, 2.48. This is used for calculating the maximum bend with equation 2.39.

$$C = \frac{L}{2n}\sqrt{1 - \sin^2\alpha} \tag{2.48}$$

3 Method

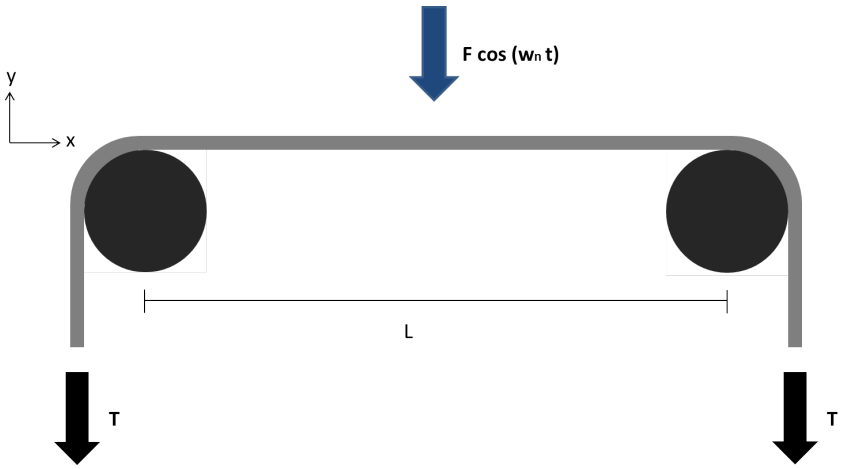

Figure 3.1: *The set-up used for the simulations. The wire is held with the tension T applied in the ends. A harmonic force with the frequency equal to the eigenfrequency is applied in the middle of the wire.*

The idea is to excite the wire with a harmonic force big enough for the wire to achieve an equal bending moment as the bending moments present in conventional wire rolls. This should give at least the same effect on the oxide scales as from the wire roll. What exactly will happen is hard to say without experiments. But the comparison between the acquired results from the MATLAB simulations and the ones from the wire rolls gives a hint if the forces are in the right order of magnitude. A schematic set-up is seen in figure 3.1.

The eigenfrequencies of the wire for different tensions and lengths have been analytically calculated. When exciting the wire with a resonant frequency the wire oscillation amplitude will be very large compared to the force applied to it and this is what is desired.

The Euler method for discretizing the wave equation is used to evaluate how the wire moves when excited by the harmonic force. The eigenfrequencies of the model are also reviewed and compared to the analytical eigenfrequencies. Different set-ups for the force have also been analyzed and evaluated and also how much amplitude the wire displacements can have for the wire not to reach plasticity which is necessary for the model to hold, this is also necessary for the wire making proceess.

Figure 3.2 shows a simulation of the wave equation. The figure shows the wire, that is set up between $x = 0$ and $x = 3\,\mathrm{m}$ with the displacement amplitude of one mm. The displacement is used to calculate the bending moment for that value of n. In the results the time-lapse of the momentum is shown in graphs.

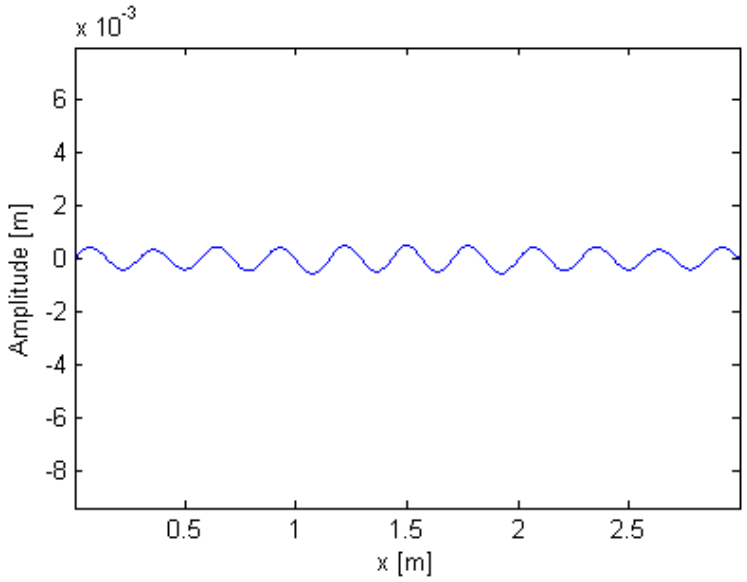

Figure 3.2: *The set-up for the bending moment simulations. Here a wire that is excited with n=21.*

4 Results

This section contains the results of the simulations in MATLAB. In the simulations values for a steel wire with the diameter 5.5 mm has been used.

4.1 Length and Tension Dependencies

The results from the simulations to determine the length dependence of the tension and frequency, is shown in figure 4.1 and 4.2 and figure 4.3 and 4.4 respectively. $n = 121$ is equal to $f = 18735$ Hz.

Figure 4.1 and the zoomed in figure 4.2 shows that in order to steer the eigenfrequencies a length of at least 3 m is needed. The eigenfrequencies are very close to each other for different tensions. For subsequent simulations a tension of 10 kN has been used.

Figure 4.3 and the zoomed in 4.4 shows how close in frequency the different eigenmodes are.

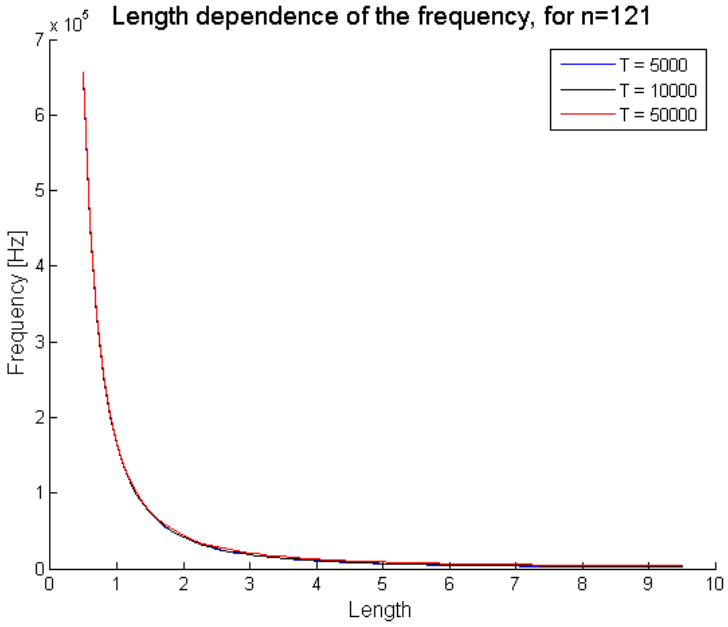

Figure 4.1: *Length dependence of the frequency for n=121 for different values of the tension.*

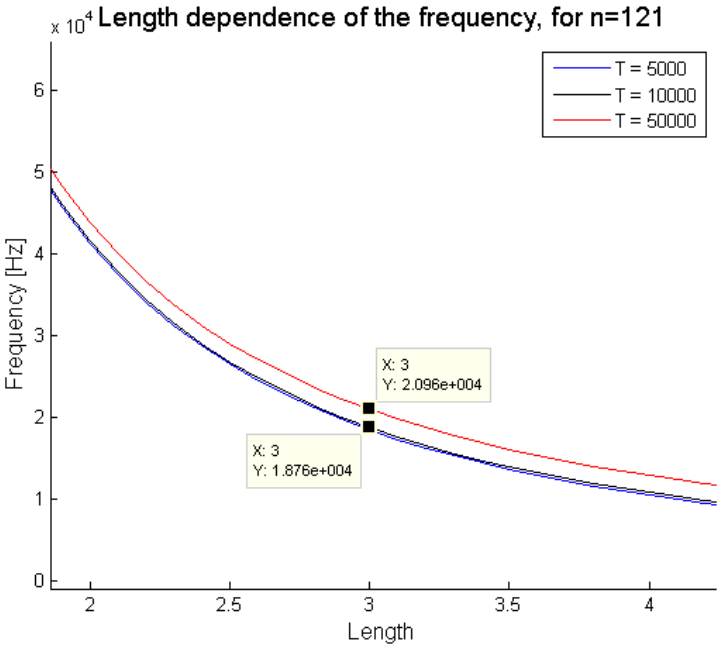

Figure 4.2: *A zoom of figure 4.1 around L=3.*

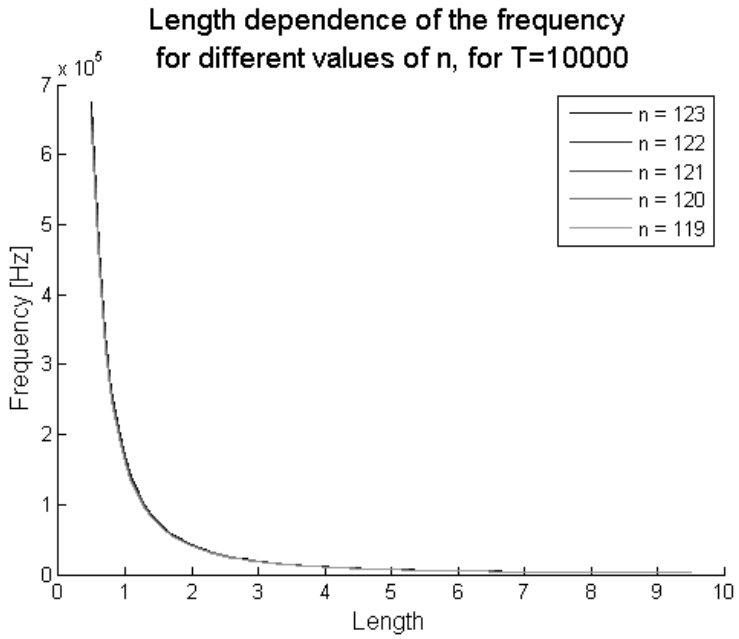

Figure 4.3: *Length dependence of the frequency for T=10000 for different values of n.*

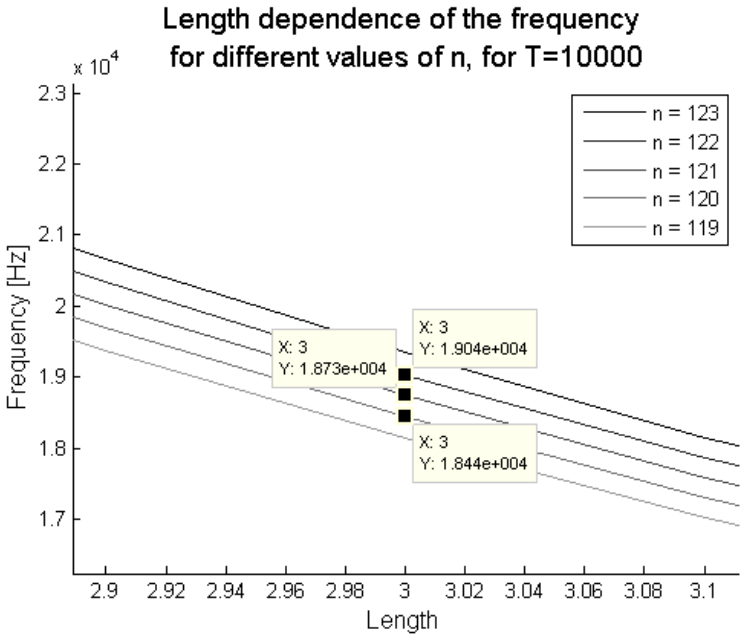

Figure 4.4: *A zoom of figure 4.3 around L=3.*

4.2 Model Eigenfrequencies

The model eigenfrequencies has been compared with the analytical eigenvalues. For the low eigenmodes the model is quite accurate but for big values of n the values diverges. The shift of the model eigenfrequencies for a thousand elements (J=1000) is seen in figure 4.5 and 4.6.

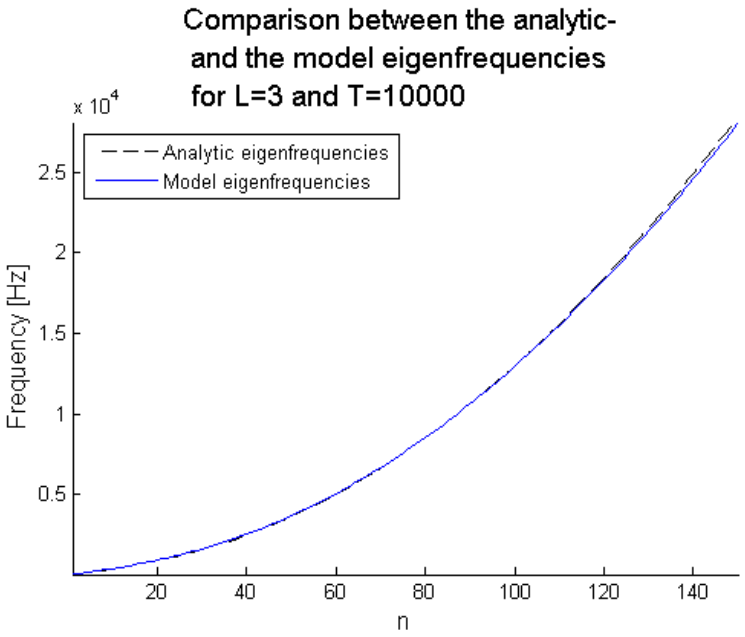

Figure 4.5: *The eigenfrequencies for different values of n.*

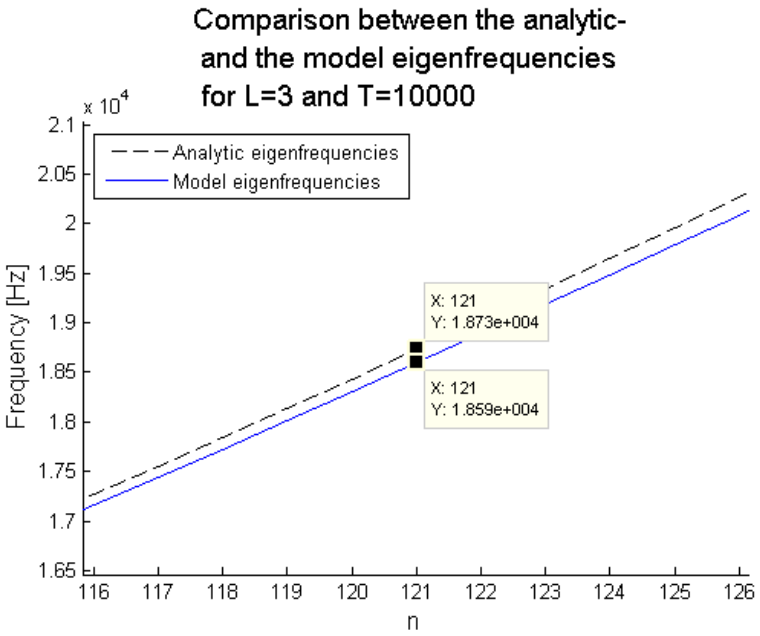

Figure 4.6: *A zoom of figure 4.5 around n=121.*

4.3 Maximum Bend for Elastic Region

In figure 4.7 the maximum possible bend for different elongations is shown.

Higher frequencies makes it possible to achieve larger bending moments by less stretching of the wire. The wire can reach a bending moment of 215 Nm at the frequency of 0.25 MHz without stretching the wire more than 0.2%.

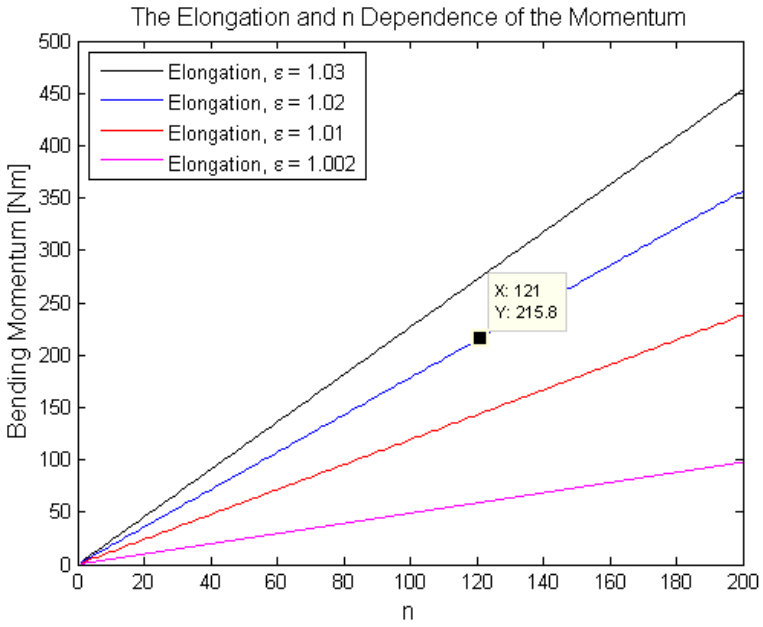

Figure 4.7: *The maximum possible bend for different frequencies, for the wire without elongating it more than ϵ. The bending moment for n=121 is 215.8 Nm.*

4.4 Wave Equation Simulations

The simulations for the wave equation contains a time-lapse over the calculated bending moment. The interesting part is the maximum value of the curve. The bending moment goes up and down with the frequency of the harmonic force because of the flattening of the wire between the maxima. When the wire oscillates close to the eigenfrequency, the amplitude of the oscillations increase.

The following section is divided into subsections where different aspects of the applied force and the model is looked in to. These are:
- The Frequency
- Constant F
- Constant p
- Constant l
- and the Matrix Size

4.4.1 The Frequency

Figure 4.8 and 4.9 shows the same set-up with the only difference being that the frequency is changed. The amplitude of the oscillations and its corresponding bending moment is much greater when the wire is excited with the eigenfrequency calculated from the model than the analytic eigenfrequency. In the following simulations the model eigenfrequency is used for $n = 121$. When changing the applied frequency to that of the previously calculated model eigenfrequecy the amplitude increases.

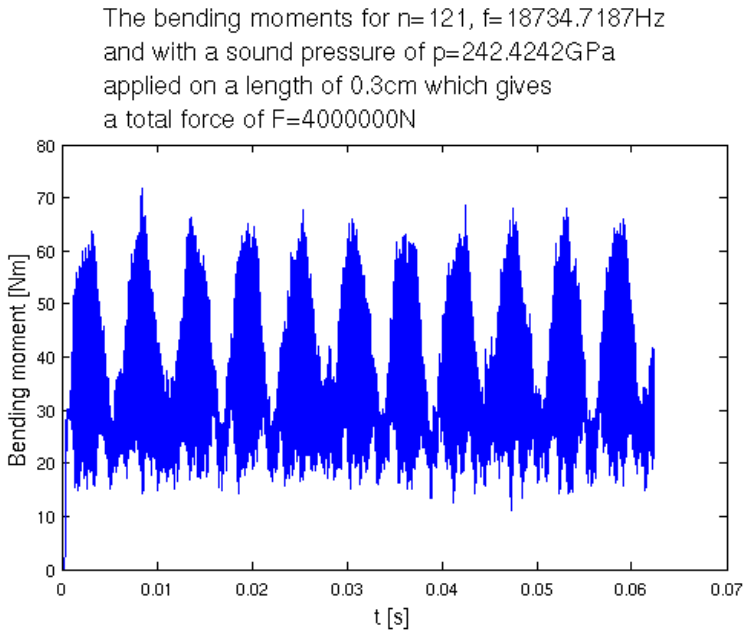

Figure 4.8: *A set-up with the analytical eigenfrequency for n=121.*

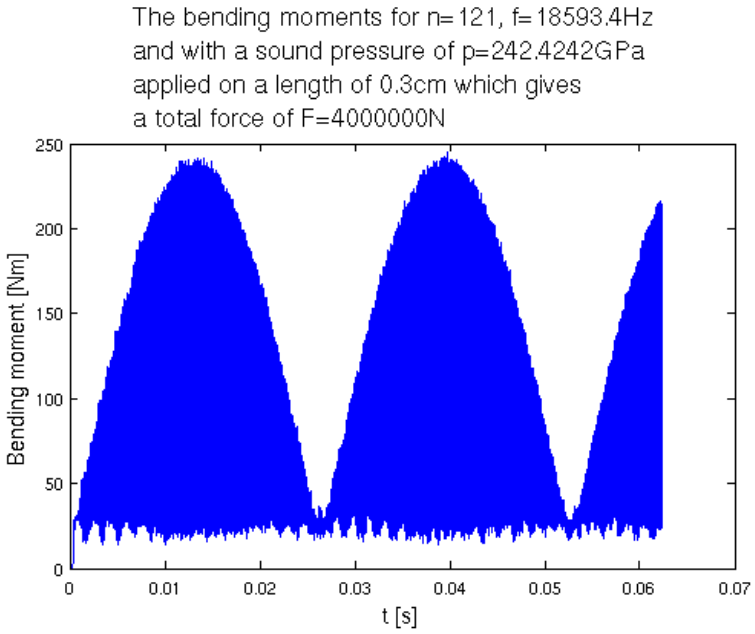

Figure 4.9: *The same set-up as figure 4.8 but with the frequency calculated for the model eigenfrequency.*

4.4.2 Constant F

A set-up with constant total force and increasing area that the force is distributed on is shown in figure 4.10, 4.11 and 4.12. When the force is distributed over a larger area the amplitude of the bending moment decreases, but less pressure is needed. When the area further inreases the efficiency drops even more.

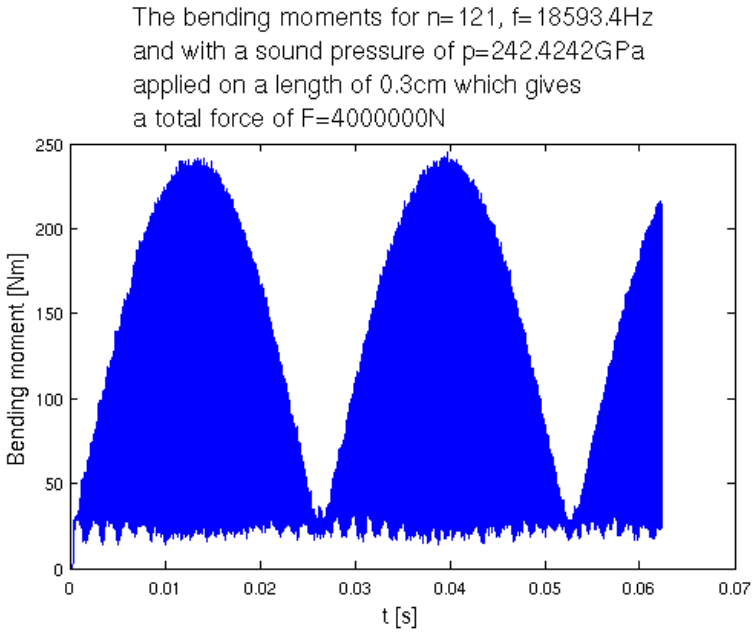

Figure 4.10: *Set-up A for constant F.*

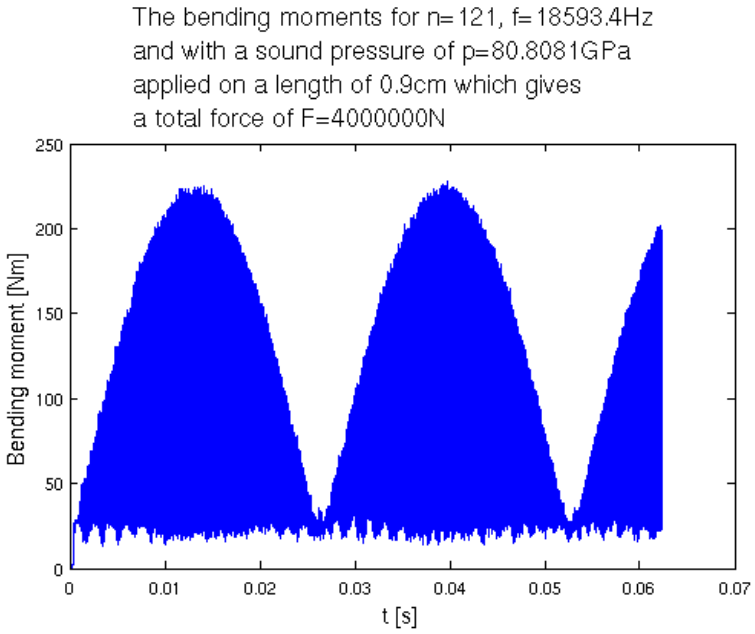

Figure 4.11: *Set-up B for constant F.*

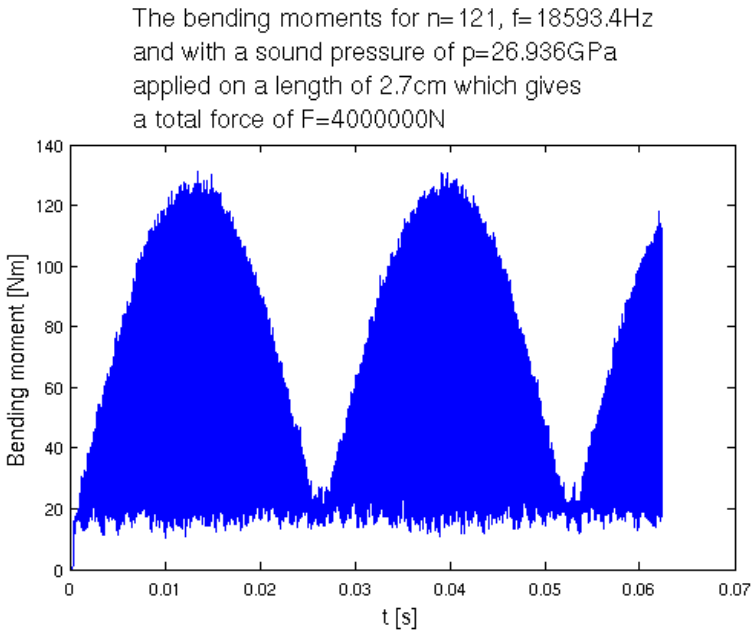

Figure 4.12: *Set-up C for constant F.*

4.4.3 Constant p

In figure 4.13, 4.14 and 4.15 the pressure is held constant. The frequency is much lower than earlier. In these figures one can see that the amplitudes are about the same for the three figures. Figure 4.15 has the lowest amplitude but by far the highest total force, the area of which the pressure is applied to is thus too large.

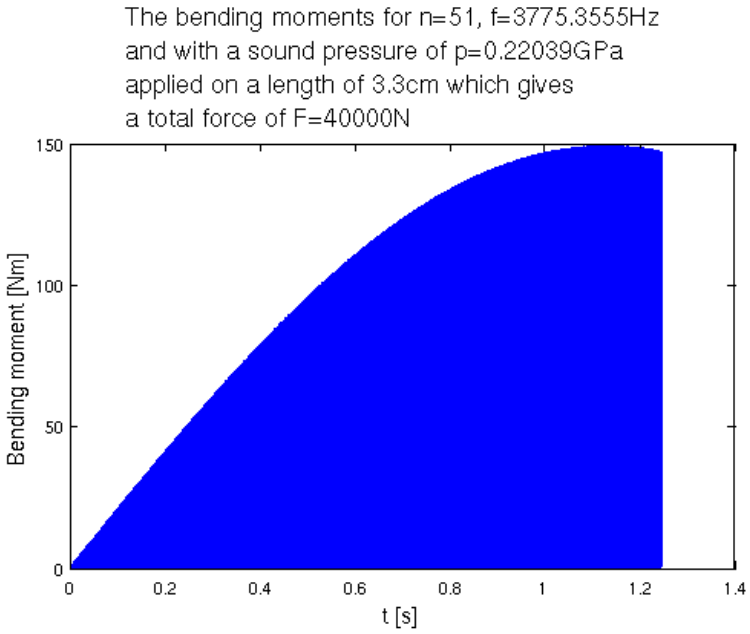

Figure 4.13: *Set-up A for constant p*

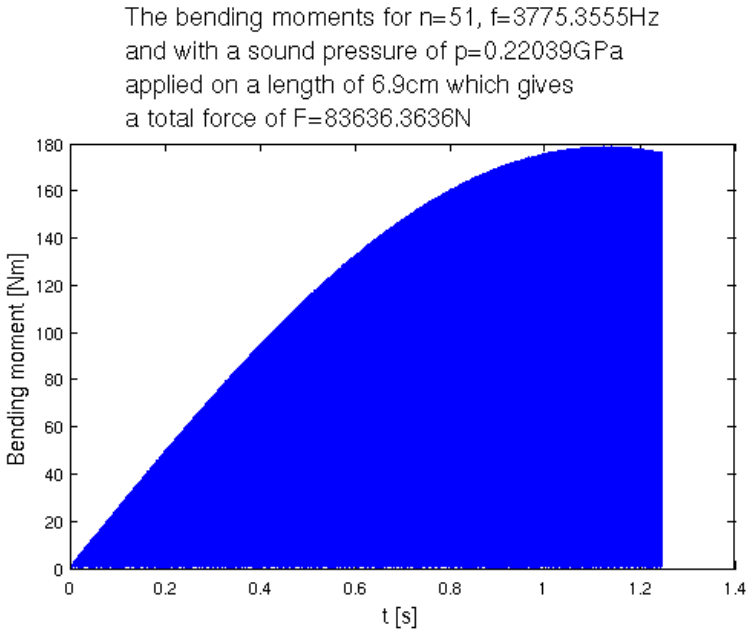

Figure 4.14: *Set-up B for constant p.*

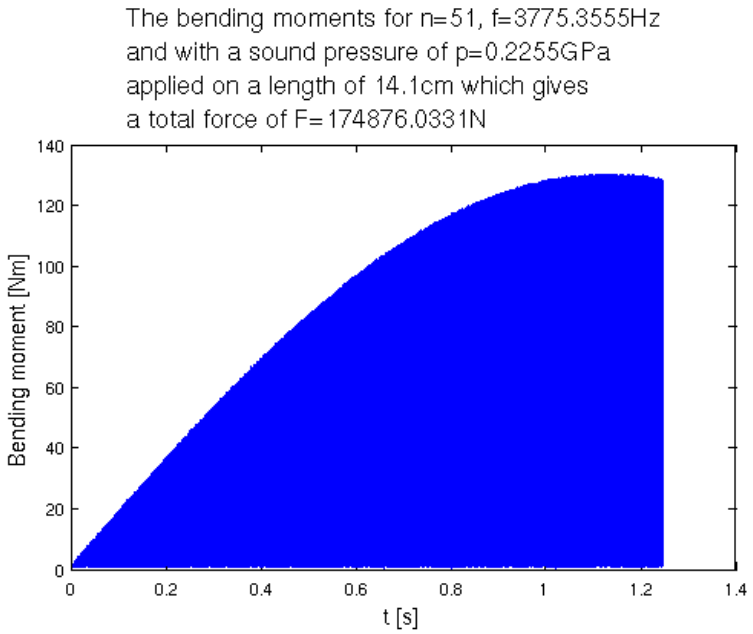

Figure 4.15: *Set-up C for constant p.*

4.4.4 Constant l

In figure 4.16 and 4.17 the length of which the force is applied to is held constant. The amplitude is directly proportional to the applied force when the lengths on which the pressure is allied to is the same.

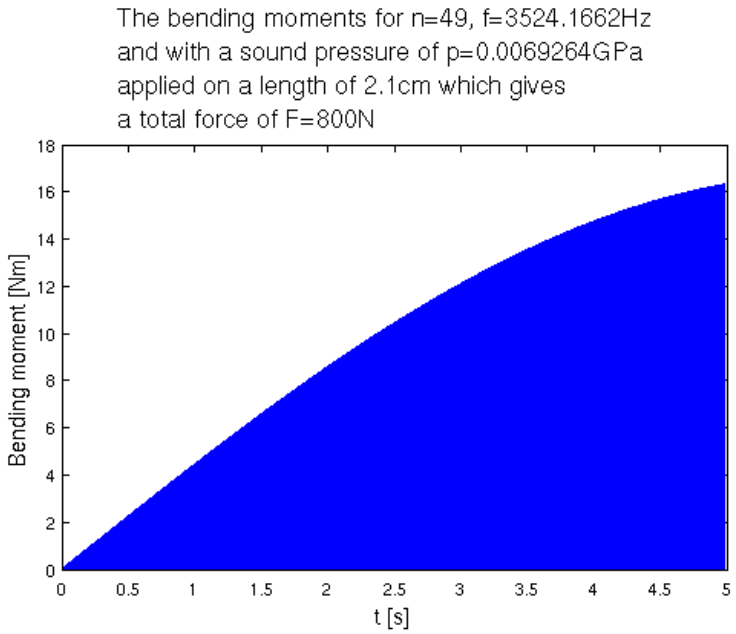

Figure 4.16: *Set-up A for constant l.*

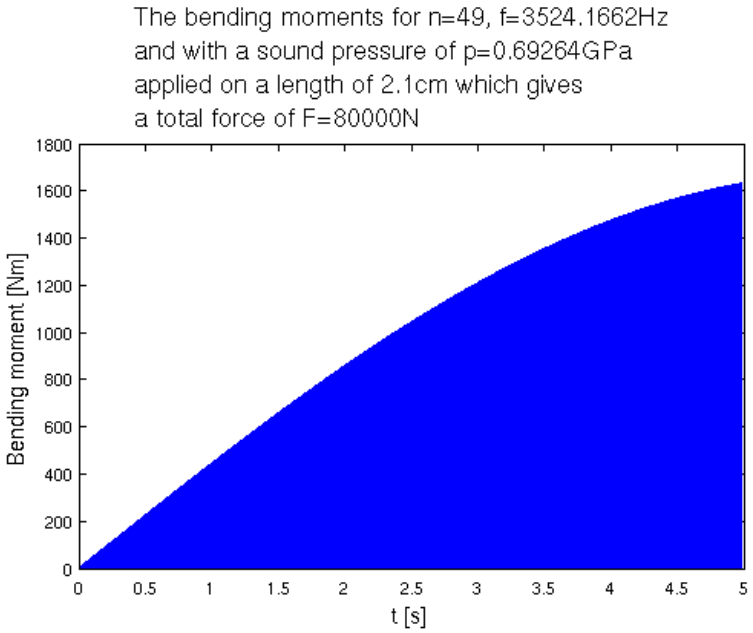

Figure 4.17: *Set-up B for constant l.*

4.4.5 Matrix Size

Here the number of elements used in the model J the difference between the simulations. $J = 1000$ in figure 4.18 and $J = 1500$ in figure 4.19. One would expect that more elements should result in a more accurate solution and therefore the model eigenfrequency would be closer to the analytical which would result in higher amplitude of the curve with more elements. This is probably due to that the time-step is too large for the bigger model but a smaller would take too long computation time.

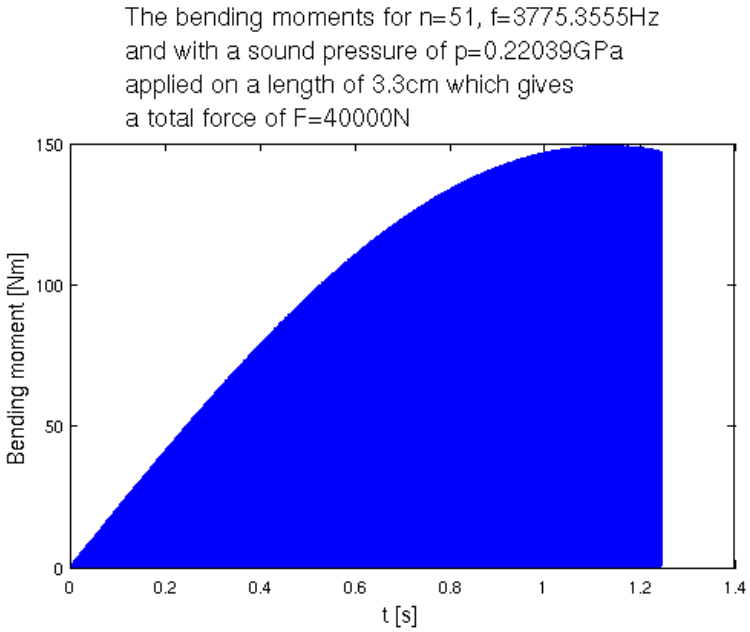

Figure 4.18: *J=1000.*

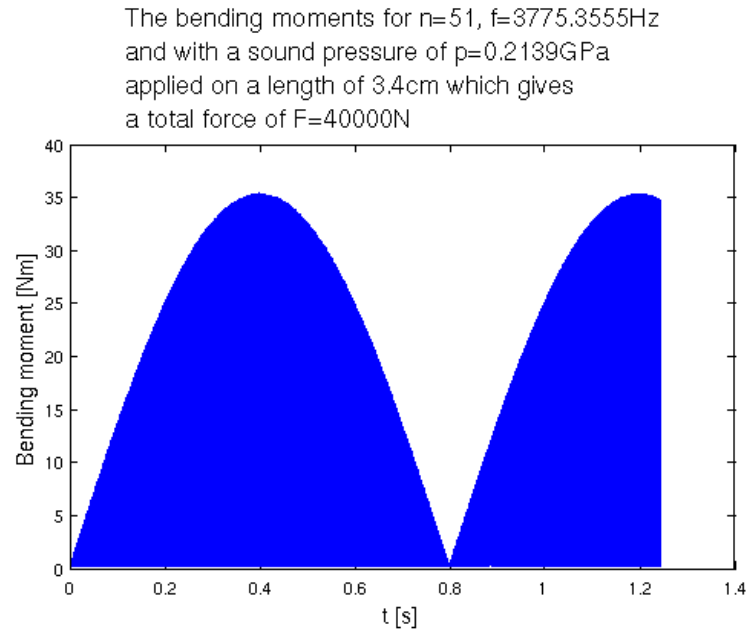

Figure 4.19: *J=1500.*

5 Discussion

Here follows a discussion of the results.

5.1 Length and Tension Dependencies

The length dependence of the eigenfrequencies shows that a set-up where the wire length is at least 3 m is desired because shorter lengths make the controllability of the eigenfrequencies much more difficult. Also, with too long wire other effects might take place such as the wire collapsing of its own weight. The tension can be selected freely with the only constraint that it must hold the wire still.

5.2 Model Eigenfrequencies

The model eigenfrequencies results show that the model is quite good for predicting the eigenfrequency, although there is a small shift in frequency especially for higher frequencies. It is possible that this affects the results for $n = 121$ in a way that the model might be insufficient for determining the correct force needed to achieve the desired amplitude.

5.3 Maximum Bend for Elastic Region

These calculation says that the frequency must be at least 18.5 kHz ($n = 121$) to achieve sufficiently large oscillations for the bending momentum to reach 215 Nm without elongating the wire more than 2%. Higher than 2% elongation can not be accepted due to plasticity. Lower frequencies can not achieve that bending moment without stretching the wire over the plasticity limit. The wire might reach plasticity already on 0.2% elongation in the radial direction, that would require the frequency to be 0.25 MHz.

5.4 Matrix Size

For the simulations, there are always one thousand elements that are evaluated, except in the section about the matrix size. The results from this section indicates that even if more positions on the wire is evaluated the result is not better. This is probably due to that the time-steps are to big and thus the bending moment becomes less than for the simulation with $J = 1000$ even though the result should be more accurate with more cells. By decreasing the time-step size the simulation time quickly becomes too long.

5.5 The Results from Constant F, p and l

From these simulations one can see that the amplitude of the wire depends on what total force is applied. If the force is spread out over a length that is longer than $\approx \frac{1}{2}$ wavelength the effect is lowered. For $n = 121$ that is $\frac{L}{2n} = 1.2$ cm and for $n = 51$ this value is 2.9 cm. From the constant l simulations one can see that the bending moment is directly

proportional to the applied force when the force is applied to a length that is shorter than the half wavelength. The simulations assumes, and only works for, an elastic wire.

5.6 The Acoutic Pressure

It is hard to exactly say how much high pressure is needed to excite the wire to needed amplitude at 18.5 kHz. Figure 4.11 shows the suggested optimal area and the bending moment reaches a bit over 230 Nm but the needed pressure is 80 GPa which is a very high pressure. For a sonic generator located 1 cm from the wire to reach a pressure of 1 GPa in water a power of 830 MW would be needed which is not achievable. It is however likely that the real value might be lower for the real wire becuase of the uncertainty of the model for the higher frequencies. When the frequency is a bit off the eigenfrequency the oscillation amplitude drops significantly.

6 Conclusion

For ultrasound cleaning to work properly the surface needs to have discontinuities for the cavitation erosion to be effective. This leads to the idea of adding an ultrasound generator acting on a small area whos function is to make the wire vibrate to loosen the scales. To add the extra ultrasound generator into the tank used for ultrasound cleaning makes additional preparations for the wire unneccessary. Using dual frequencies for eroding the oxide and cleaning the wire as suggested by Kohli and Mittal may erase the need for after work. The Stelmor cooling process should also be optimized for minimizing the hematite layer. It is uncertain exactly how much power the ultrasound generator needs to emit to successfully vibrate the wire with sufficient amplitude. The effects from cavitation known from the concept of ultrasound cleaning may add additional pressure, the effect from this is not included in this work.

6.1 Future Work

A future work to evaluate the concept in practice would be a very interesting task and needed to be able to validate the results and also to be able to see how much pressure that is possible to attain at the surface of the wire.

References

[1] Per Enghag. *Trådteknik*. Materialteknik, Örebro, Sweden, 2010.

[2] A. Chattopadhyay et al. Study on formation of "easy to remove oxide scale" during mechanical descaling of high carbon wire rods. *Surface & Coatings Technology*, 203:2912–2915, 2009.

[3] Rajiv Kohli and Kashmiri L. Mittal. *Developments in Surface Contamination and Cleaning – Particle Deposition, Control and Removal*. Elsevier Inc., Amsterdam, Netherlands, 2009.

[4] Peter Olsson. *Svängningar och Ljudutbredning, Del 1: Endimensionella System*. Avdelning Mekanik CTH, Göteborg, Sweden, 1989.

[5] Hans Lundh. *Grundläggande hållfasthetslära*. Kungliga tekniska högskolan. Institutionen för hållfasthetslära, Stockholm, Sweden, 2007.

[6] Gerald B. Folland. *Fourier analysis and its applications*. Wadsworth & Brooks/Cole, Pacific Grove, California, 1992.

[7] Singiresu S. Rao. *Mechanical Vibrations, 4th edition*. Pearson Education, Inc, Upper Saddle River, New Jersey, 2004.

[8] Lennart Råde and Bertil Westergren. *Mathematics Handbook*. Studentlitteratur, Lund, Sweden, 2008.